International Journal of Power Electronics and Drive System (IJPEDS)
Vol. 7, No. 3, September 2016, pp. 701~712
ISSN: 2088-8694, DOI: 10.11591/ijpeds. v7.i3.pp701-712

Solar Photovoltaic Generators with MPPT and Battery Storage in Microgrids

B.V Rajanna[1], SVNL Lalitha[2], G Joga Rao[3], S.K Shrivastava[4]
[1,2] Department of Electrical and Electronics Engineering, KL University, India
[3,4] Department of Electrical and Electronics Engineering, SunRise University, India

Article Info

Article history:

Received Nov 12, 2015
Revised Mar 13, 2016
Accepted Apr 14, 2016

Keyword:

Distributed generation
Islanded operation
MATLAB/Simulink
Micro-Grids
MPPT
PV system

ABSTRACT

Maximum power point tracking (MPPT) of a photo voltaic system with different temperature and insolation conditions used for Micro grids can be explained in this paper. The different steps of the design of this controller are presented together with its simulation and the feasibility of control methods to be adopted for the operation of a micro grid when it becomes isolated. Normally, the micro grid operates in interconnected mode with the medium voltage network; however, scheduled or forced isolation can take place. In such conditions, the micro grid must have the ability to operate stably and autonomously. An evaluation of the need of storage devices and load to take off strategies is included in this paper. Solar photovoltaic (PV) energy has witnessed double-digit growth in the past decade. The penetration of PV systems as distributed generators in low-voltage grids has also seen significant attention. In addition, the need for higher overall grid efficiency and reliability has boosted the interest in the microgrid concept. High-efficiency PV-based microgrids require maximum power point tracking (MPPT) controllers to maximize the harvested energy due to the nonlinearity in PV module characteristics. This paper proposes an approach of coordinated and integrated control of solar PV generators with the maximum power point tracking (MPPT) control and battery storage control to provide voltage and frequency (V-f) support to an islanded microgrid. The simulation studies are carried out with the IEEE 13-bus feeder test system in grid connected and islanded microgrid modes. The MPPT of a Photovoltaic System for Micro Grid operation is successfully designed and simulated by using MATLAB/Simulink Software in this paper.

Corresponding Author:

BV Rajanna,
Department of Electrical and Electronics Engineering,
KL University, Green Fields,Vaddeswaram,
Pincode: 522502, Guntur District, A.P., India.
Email: bv.rajanna@gmail.com

1. INTRODUCTION

The microgrid is a collection of distributed generators or microresources, energy storage devices, and loads which operate as a single and independent controllable system capable of providing both power and heat to the area of service [1]. The microresources that are incorporated in a microgrid are comprised of small units, less than 100 kW, provided with power electronics (PE) interface. Most common resources are Solar Photovoltaic (PV), Fuel Cell (FC), or microturbines connected at the distribution voltage level. In a micro grid, the micro sources and storage devices are connected to the feeders through the micro source controllers (MCs) and the coordination among the micro sources is carried out by the central controller (CC) [2]. The micro grid is connected to the medium voltage level utility grid at the point of common coupling (PCC) through the circuit breakers. When a micro grid is connected to the grid, the operational

control of voltage and frequency is done entirely by the grid; however, a micro grid still supplies the critical loads at PCC, thus, acting as a PQ bus. In islanded condition, a micro grid has to operate on its own, independent of the grid, to control the voltage and frequency of the micro grid and hence, acts like a PV (power-voltage) bus. The operation and management in both the modes is controlled and coordinated with the help of micro source controllers (MCs) at the local level and central controller (CCs) at the global level. Similar to the traditional synchronous generator frequency control [3], the micro grid voltage and frequency control can also be performed using droop control methods [4]–[8]. The present work provides fast response characteristics for voltage and frequency control as compared to the secondary control considered in [8]. The analogy between inverter control and the synchronous generator control in an islanded micro grid is studied in detail in [9].

In the islanded mode, there is the necessity of having a reference voltage and frequency signals in the micro grid inverter control [10]. The operation and control of the inverter interface of renewable- based distributed energy resources (DERs), like Solar Photovoltaic (PV) in a micro grid, is a real challenge, especially when it comes to maintaining both micro grid voltage and frequency within an acceptable range. A voltage control method based on traditional droop control for voltage sag mitigation along with voltage ride through capability is proposed in [11]. A dynamic voltage regulation based on adaptive control is proposed in [12], [13]. However, there are not many researches works performed on V-f or P-Q control using solar PV including MPPT control and battery storage in micro grids. In [14], frequency regulation with PV in micro grids is studied; however, this work does not consider the voltage control objective and lacks battery storage in the micro grid. In [15], a small scale PV is considered in a grid-connected mode to control the active and reactive power of the system. Here, the control methods consider abc-dq0 transformation and vice versa which is avoided in the present paper. In [16], power modulation of solar PV generators with an electric double layer capacitor as energy storage is considered for frequency control. In [17], load frequency control is implemented in micro grid with PV and storage; however, this work also lacks the consideration of a voltage control objective.

The voltage and frequency control with solar PV and battery in micro grid with an induction machine is investigated in [18]; however, this work does not explain the transfer mechanism of controls to consider the battery SOC constraint. In summary, the previous works in this topic either lack the incorporation of an energy storage component or the voltage control objective along with frequency control or the incorporation of control transition in different scenarios. The present work fulfills these gaps by considering all of these objectives [19]. The coordinated control and management of distributed generators and renewable energy resources together with controllable loads and storage systems are the most important and challenging tasks in micro grid operation [20], [22]. Micro grid can be operated in grid-connected mode or in islanded mode [23]. Typically, energy storage systems are repeatedly proposed to support frequency and voltage control of micro grids. Due to the intermittency in renewable power generation and constantly changing load demand, charging and discharging of various energy storage systems in a micro grid needs to be appropriately coordinated. In islanded mode, the main responsibility of the storage is to perform energy balance. In grid-connected mode, the main goal is to prevent propagation of the renewable source intermittency and load fluctuations to the grid. In a renewable powered micro grid, a single type of energy storage systems cannot perform all these tasks efficiently. Hence, in intermittent nature of renewable energy sources, demands involve usage of storage with high energy density. At the same time, quick fluctuation of load demands requires storage with high power density. This project proposes a distributed energy storage system that contains both high energy density storage systems as well as high power density storage systems to meet the ever growing requirements. The effectiveness of the proposed approach is validated by various simulation results using HOMER software.

Nomenclature

$v_t(t)$	Instantaneous PCC voltage
$V_t(t)$	Average PCC voltage
$v_C(t)$	Instantaneous inverter output voltage
$V_C(t)$	Average inverter output voltage
L_C	Coupling inductor
P(t)	Inverter average active power
Q(t)	Inverter average reactive power
S(t)	Inverter average apparent power
δ^*	Duty cycle of DC/DC booster
P_{MPPref}	Reference maximum power
P_{PV}	PV active power output

α_1^*	Phase shift between $v_C(t)$ and $v_t(t)$
f_{ref}	Reference microgrid frequency
$f_{measured}$	Measured microgrid frequency
P_{AC}	AC side total average active power
P_{DC}	DC side average active power
$P_{Battref}$	Reference battery active power
P_{Batt}	Actual injected battery active power
Q_{ref}	Average reactive power reference (Reactive Load)
Q_{actual}	Actual generated reactive power
P_{ref}	Average active power reference (Active Load)
P_{actual}	Actual generated active power

2. PROPOSED METHOD

2.1. Solar PV Modeling and Validation

The commonly accepted solar cell model is a one diode model [19]. This work uses the single diode model of the solar cell to model the Kyocera KC200GT solar array, which is shown in Figure 1. The I-V characteristics of a solar array, as shown in Figure 2, are represented by (1).

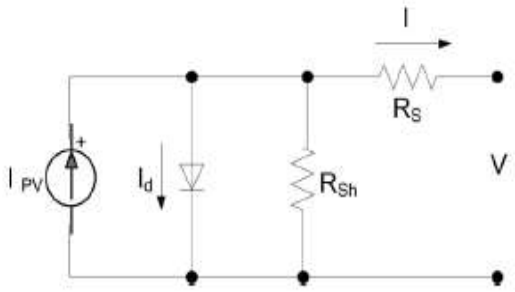

Figure 1. One diode equivalent circuit of Solar PV

$$I = I_{pv} - I_0\left(e^{\left(\frac{V+R_sI}{V_{therm}\alpha}\right)} - 1\right) - \frac{V+R_sI}{R_{sh}} \quad (1)$$

where I_{pv} and I_0 are the photo current and the diode saturation currents respectively. The photocurrent of the PV array depends linearly on the solar irradiation and the cell temperature. Where I_{pv} and I_0 are the photo current and the diode saturation currents respectively. The photocurrent of the PV array depends linearly on the solar irradiation and the cell temperature. Vtherm (=NskT/q) is the thermal voltage of the array, Ns being the cells connected in series for greater output voltage, K is the Boltzmann constant (1.3806503X10-23 J/K), T is the temperature of the p-n junction of the diode q (1.60217646 X 10-19) is the electron charge Rs and Rsh are the equivalent series and shunt resistances of the array respectively and α is the ideality factor usually chosen in the range $1 \leq \alpha \leq 1.5$. Here α is taken as 1. The photocurrent of the PV array depends linearly on the solar irradiance and the cell temperature, as shown by (2).

$$I_{pv} = \left(I_{pv,n} + K_I\Delta T\right)\frac{G}{G_n} \quad (2)$$

Here, $I_{pv,n}$ is the photocurrent at the standard test condition (STC, 250C and 1000 W/m2), K_I is the short circuit current/temperature coefficient, ΔT is the difference between the actual and nominal temperature in Kelvin, G is the irradiation on the device surface and G_n is the nominal radiation, both in W/m^2. $I_{pv,n}$ Can be calculated based on

$$I_{pv,n} = \frac{R_{sh}+R_s}{R_{sh}} I_{SC} \quad (3)$$

Using these fundamental equations and parameters from the data sheet, the PV model is developed and verified with the panel datasheet. The I-V characteristics of KC200GT for different irradiance levels at

the cell temperature of 250C and varying cell temperature for a constant irradiance level of 1000 W/m2 as obtained from the simulation are shown in Figures 2(a) and (b), respectively.The similarities of the I-V curves for different conditions with the corresponding curves in the KC200GT panel datasheet prove thevalidity of the developed solar panel model. The parameters of the PV panel under study are shown in Table 1.

Table 1. PV Panel Parameters at 1000 W/M and 25 C

Model	Kyocera KC200GT
P_{MPP}	200W
V_{MPP}	26.30V
I_{MPP}	7.61A
V_{OC}	32.90V
I_{SC}	8.21A

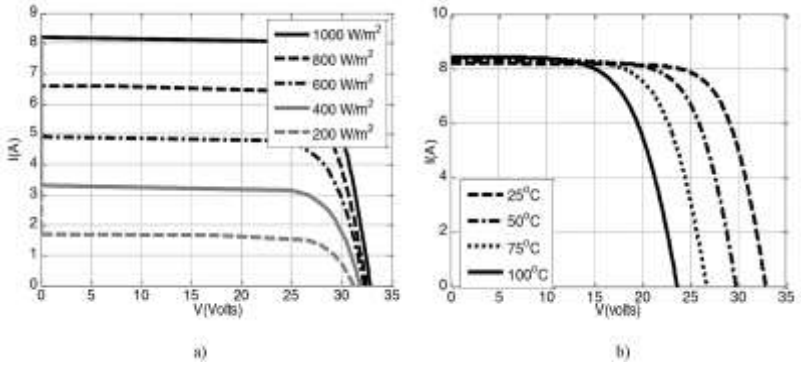

Figure 2. The-characteristics of Kyocera KC200GT from simulation with (a) varying irradiance at a cell temperature of 25 C and (b) varying cell temperature at 1000W/m.

The PV system under study for the proposed V-f and P-Q control has 125 strings with each string having 4 series connected panels. The Maximum Power Point (MPP) for a single panel of KC200GT at 1000 W/m2 and 250C (STC) is 200 W. Hence, the maximum power of the PV generator at STC is 125 X 4 X 200 =100kW. But the MPP varies according to the change in irradiance level and cell temperature.

3. RESEARCH METHOD

3.1. PV System Configuration and System Description

3.1.1. PV System Configuration

Figure 3 shows the PV system configuration for V-f and P-Q control with PV operating at MPP including the battery storage backup. It is a two-stage configuration where a DC-DC boost converter is used for MPPT control. The system also considers a battery back-up in case of emergencies while maintaining the voltage and frequency of the microgrid or while trying to supply the critical loads. A battery is connected in parallel to the PV to inject or absorb active power through a bidirectional DC-DC converter. When the battery is absorbing power, the converter operates in the buck mode and when battery is injecting power to the grid, it operates in the boost mode. The operation mode is maintained through the control signal provided to the converter switches. The PV system is connected to the grid through a coupling inductor L_C. The coupling inductor filters out the ripples in the PV output current. The connection point is called the point of common coupling (PCC) and the PCC voltage is denoted as $V_c(t)$. The rest of the system in Figure 3 denotes the IEEE 13-bus distribution feeder which is simplified as a substation with the feeder equivalent impedance, R+jwL_s. The PV source is connected to the DC link of the inverter with a capacitorC_{dc}. The PV is the active power source, and the capacitor is the reactive power source of the PV system. According to the instantaneous power definitions for a balanced three-phase system consider $V_t(t)$ and $V_c(t)$ denote the instantaneous PCC voltage and the inverter output voltage (harmonics neglected) respectively, then the average power of the PV denoted as P(t), the apparent power S(t) and the average reactive power Q(t) of the PV are as given by equations (4)-(6).

$$P(t) = \frac{2}{T}\int_{t-\frac{T}{2}}^{t} V_t(T) i_C\,(T)dt = \frac{V_t(t)V_C(t)}{WL_C}\sin\alpha \quad (4)$$

$$S(t) = V_t(t)I_C(t) = \frac{V_t(t)}{\omega L_C}\sqrt{V_t(t)^2 + V_C(t)^2 - 2V_t(t)V_C(t)\ \cos\alpha} \quad (5)$$

$$Q(t) = \sqrt{S^2(t) - P^2(t)} = \frac{V_t(t)}{\omega L_C}\left(V_C(t)\ cos\,\alpha - V_t(t)\right) \quad (6)$$

Here, α is the phase angle of V_C(t) relative to the PCC voltage. P (t) and Q (t) in (4) and (6) can be approximated by the first terms of the Taylor series if the angle α is small, as shown in (7) and (8):

$$P(t) \approx \frac{V_t(t)V_C(t)}{WL_C}\alpha \quad (7)$$

$$Q(t) \approx \frac{V_t(t)}{\omega L_C}(V_t(t) - V_C(t)\,) \quad (8)$$

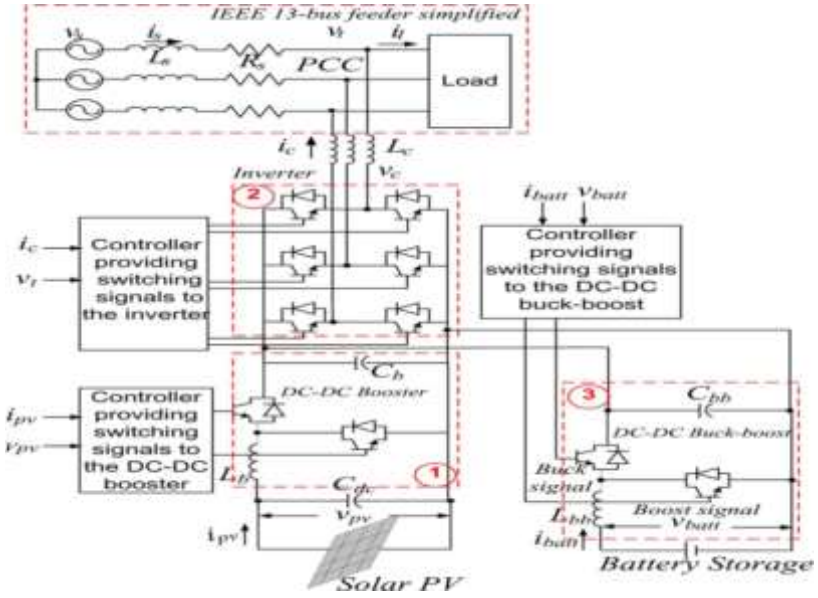

Figure 3. System configuration of V-f control with solar PV generator operating at MPPT with a battery storage system

3.1.2. Battery Modelling

In this paper, the battery model is taken from the MATLAB SimPower Systems library with appropriate parameters which will be used for the proposed V-f and P-Q controls. The detailed description about the battery model is given in [21]. It is assumed that the lead acid battery can be discharged up to SOC of 20% and can be charged up to SOC of 80%. The battery model in [21] is an analytical model with two equations representing the battery discharge and charge models. The battery discharge and charge model for a lead acid battery is given by equations (9) and (10), respectively.

$$V_{Batt} = V_0 - R.i - K\frac{Q}{Q-it}(it + t^*) + Exp(t) \quad (9)$$

$$V_{Batt} = V_0 - R.i - \left[K\frac{Q}{it-0.1Q}\right]i^* - \left[K\frac{Q}{Q-it}\right].it + Exp(t) \quad (10)$$

where V_{Batt} is the battery voltage (V), V0 is the battery constant voltage (V), K is polarization constant (V/Ah) or polarization resistance Q is battery capacity (Ah), $it = \int i\,dt$ battery charge (Ah), A is exponential zone amplitude (V), B is exponential zone time constant inverse (Ah), R is the internal resistance is battery current (A), i and is filtered current (A). The size of the battery is selected to provide a maximum backup

power to compensate for the PV generation in the case of a very small or no irradiance level. In this work, the MPP of PV generator at STC is 100 kW. Hence, the battery is chosen to provide this amount of power for a maximum of 1 hour with an energy content of 100 kWh. The battery backup is considered for short duration applications like frequency control and supplying power to critical loads in the event of emergency situations One hour of battery backup is considered to be enough for other backup generators to take over the controls in the microgrid emergency situations.

3.1.3. Description of IEEE 13-Bus Distribution Feeder

The diagram of the IEEE 13-bus distribution test system is shown in Figure 4. It consists of a substation, 13 buses or nodes, 11 line sections, and 8 loads. The loads comprise of a combination of constant impedance, constant current, and constant power (ZIP) loads but most of them are constant power loads. The substation is at 115 kV and it is stepped down to 4.16 kV by a distribution transformer (T1). There is one more transformer (T2) which steps down 4.16 kV to 480 V. In the grid connected mode, the substation located atBus 650 at 115 kV level is considered as a source. In an islanded microgrid case, a diesel generator connected at the same bus supplies the microgrid with a fixed amount of active power as referenced by the central controller (CC) of the microgrid.

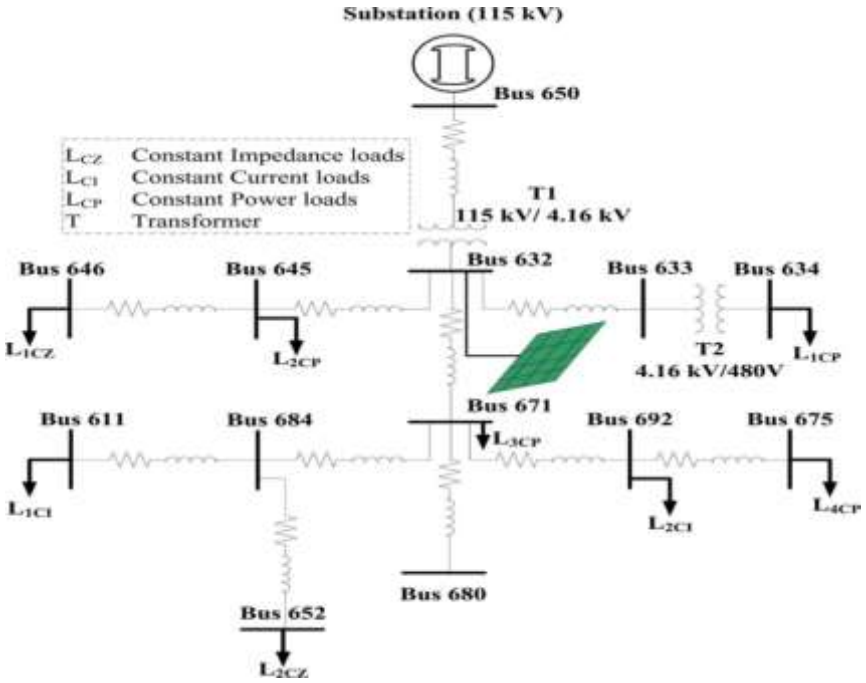

Figure 4. IEEE-13 bus distribution feeder

3.2. MPPT and Battery Integrated V-F and P-Q Conrol Methods

3.2.1.MPPT and Battery Integrated V-f Control Method

The MPPT and battery integrated V-f control diagrams are shown in Figures 5 and 6, respectively. The control comprises of one loop for MPPT control, two different loops for V-f control at the inverter side and another loop for battery power management.

The loop 1 in Figure 5 is a MPPT control. The actual PV power output, P_{PV} is compared with the MPP reference, P_{MPPref} from the look up Table 1 of irradiance versus MPP and this error is fed to a PI controller, PI_1 which outputs the duty cycle δ* for the DC-DC booster so that the array always operates at the referenced point by changing this duty cycle. The equation for this control loop is given by equation (11). Here, Kp_1 and Ki_1 are the controller proportional and integral gains respectively for this control loop.

$$\delta^* = K_{p1} * \left(P_{MPPref} - P_{PV}\right) + K_{i1} * \int_0^t \left(P_{MPPref} - P_{PV}\right) dt \quad (11)$$

Another feedback PI controller is used for voltage control at AC side. As shown in the control diagram in Figure 5 (loop 2), the PCC voltage is measured and the rms value of is $V_t(t)$ calculated. Then, the rms value $V_t(t)$ is compared to a voltage reference $V_t^*(t)$ which could be a voltage specified by the utility, and the error is fed to a PI controller. The inverter output voltage $V_C(t)^*$ is controlled so that it is in phase with the PCC voltage, and the magnitude of the inverter output voltage is controlled so that the PCC voltage is regulated at a given level $V_t^*(t)$. The control scheme can be specifically expressed as equation (12).

$$V_{C1}^*(t) = V_t(t)\left[1 + K_{P2}(V_t^*(t) - V_t(t)) + K_{I2}\int_0^t \left((V_t^*(t) - V_t(t))dt\right)\right] \quad (12)$$

where K_{P2} and K_{I2} are the controller gains for this loop. In (12), 1 has been added to the right-hand side such thatwhen there is no injection from the PV generator, the PV output voltage is exactly the same as the terminal voltage. The frequency control is carried out by controlling the active power output at the inverter side as shown in the outermost loop 3. The referenced microgrid frequency of 60 Hz is compared with the measured value and this error is fed to the PI controller P_{I3} that provides the phase shift contribution α_1^* which shifts the voltage waveform in timescale such that the active power injected will be enough to maintain the frequency at 60 Hz nominal value. The equation for this control is given by (13).

$$\alpha_1^* = K_{P3}\left(f_{ref} - f_{measured}\right) + K_{I3}\int_0^t \left(f_{ref} - f_{measured}\right) dt \quad (13)$$

There is another controller P_{I4} used in the same loop 3. This controller maintains active power balance between the AC and DC sides of the inverter. The reference signal for P_{I4} is obtained from the dynamically changing active power injection from the inverter at the AC side as determined by the output of P_{I3}. Themeasured AC side active power $P_{ACmeasured}$ is multiplied by a factor of 1.02 considering the efficiency of inverter as 98% such that the DC side active power is 102% of the AC side active power. The DC side active power is compared with this value of AC side power and the error is fed to P_{I4} to obtain the phase shift contribution from this loop as α_2^*. The equation for this control is given by (14).

$$\alpha_2^* = K_{P4}(1.02 * P_{AC} - P_{DC}) + K_{I4}\int_0^t (1.02 * P_{AC} - P_{DC})\, dt \quad (14)$$

The phase shift contributions from DC and AC sides, α_1^* and α_2^* are then averaged as given by (15) to obtain the final phase shift, α^* of the voltage waveform, V_{C1*} which, then, generates the voltage reference signal V_{C*} for the inverter PWM.

$$\alpha^* = (\alpha_1^* + \alpha_2^*)/2 \quad (15)$$

Here, the reason behind considering phase shift contributions from both DC and AC side active power is to control the DC side voltage and achieve the desired value. By making α_1^* and α_2^* close in range through the controller gains, it can be assured that the active power at the DC and AC sides is balanced. This, coupled with the voltage control loop, assures that the DC side voltage is maintained at the value desired by the AC side voltage. The controls shown in the diagram of Figure 5 and described above are also integrated with the battery power control shown in Figure 6. The battery is incorporated in the PV system configuration in order to supply or absorb active power and support the frequency control objective with the PV generator. If there is abundant solar power and the active power required for frequency control is less than PV MPP, then the battery will be charged. If there is not enough solar power available and if the active power required for frequency control is more than PV MPP, then the battery will supply the deficit power in order to maintain the microgrid frequency at 60 Hz. Hence, the control method for the battery charge/discharge that depends on this requirement is developed as shown in Figure 6. It also shows the selection of charge and discharge modes which handle the battery SOC constraint and will be described later in the Part B of this section. In Figure 6, the reference power to the battery $P_{Battref}$ is generated dynamically by subtracting the inverter active power injection, $P_{inverter}$ from the power generated by PV, P_{PV}. The controller comprised of a PI controller, P_{I5} which receives the error signal obtained after subtracting the actual battery power, P_{Batt} from the battery reference, $P_{Battref}$. The signal obtained from P_{I5} is then compared with a triangular waveform of unity magnitude to generate the signal, S^*. This is similar to common Pulse Width Modulation (PWM) in inverter controls. K_{P5} and K_{I5} are the proportional and integral gains respectively. The equation for this control is given by (16).

$$S^* = K_{P5}\left(P_{Battref} - P_{Batt}\right) + K_{I5}\int_0^t \left(P_{Battref} - P_{Batt}\right)dt \quad (16)$$

One more step is considered to differentiate the charging and discharging mode of the battery. This is undertaken by comparing P_{PV} with $P_{inverter}$. If $P_{PV} >= P_{inverter}$, the battery is in charging mode, hence, the signal obtained from the PWM, S^* and the result of this comparison is passed through a logical AND to generate a switching signal which activates the Buck mode of the DC-DC converter. If the condition $P_{PV} >= P_{inverter}$ is false, (i.e., $P_{PV} < P_{inverter}$), the opposite of this signal and S^* is passed through a logical AND to generate a switching signal which activates the Boost mode of the DC-DC converter. Hence, with this control logic, the converter is capable of operating in both directions and therefore, effectively charging and discharging the battery whenever required. This will be verified through the results presented in Section 4 of this paper.

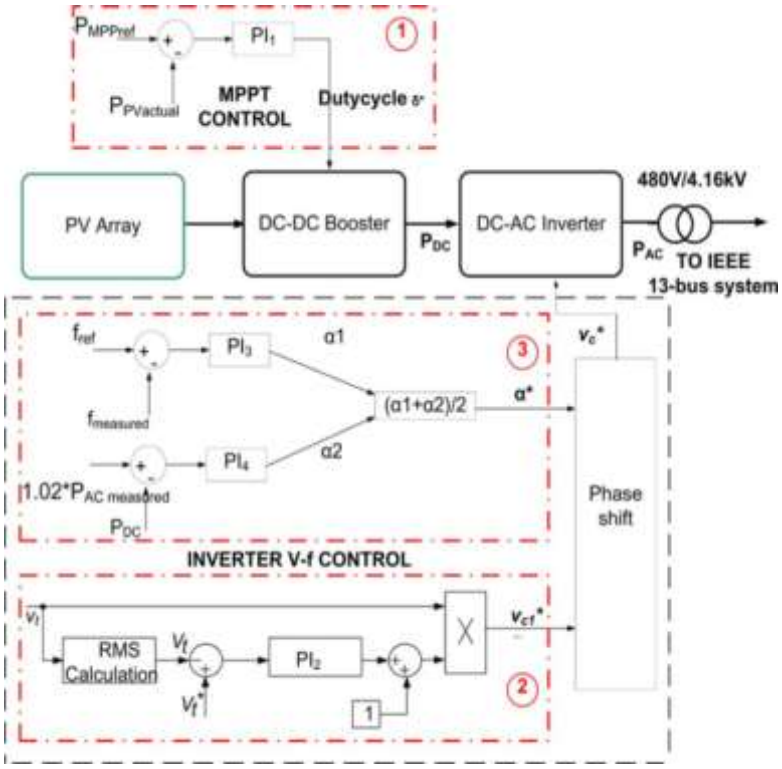

Figure 5. Integrated Solar PV MPPT and V-f control diagram

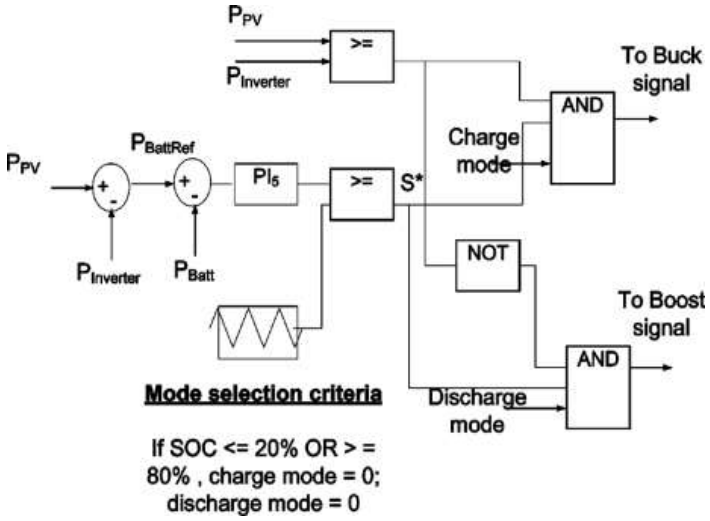

Figure 6. Battery power control diagram

4. SIMULATION RESULTS AND DISCUSSIONS

This section presents the simulation results obtained with applications of the proposed control methods to the IEEE 13-bus distribution feeder. First, the results obtained from the coordinated V-f control are presented which is followed by the results from the coordinated P-Q control. In grid connected mode, the distribution feeder is considered to be supplied by a central generator with a substation at Bus 650 at 115 kV level and a PV generator at Bus 632. Hence, in an islanded case, the distribution feeder is supplied by a diesel Generator and a PV connected at Buses 650 and 632, respectively. The Simulink diagram of the MPPT integrated with Battery of a Photovoltaic System for Micro Grid operation is shown in Figure 7.

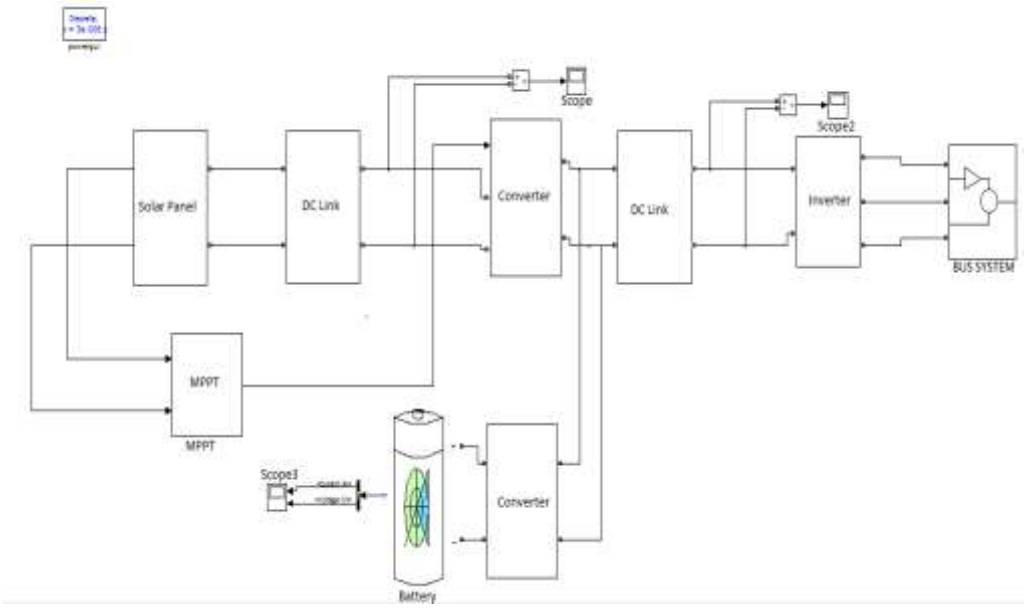

Figure 7. The Simulink diagram of the MPPT integrated with Battery of a Photovoltaic System for Micro-Grid operation

4.1.1. Test of V-F Control in Microgrid Mode:

For the demonstration of the V-f control algorithm, two different irradiance cases are considered: Case 1 with irradiance 1000 W/m2 and Case 2 with 750 W/m2. The PI controller gain parameters for Case 1 are given in Table 2. The controller gains should be adjusted slightly for the change in irradiance. While moving from the grid connected to microgrid mode, the diesel generator is controlled to generate a fixed amount of active power according to the command from the central controller. The diesel generator produces a fixed amount of 1.25 MW throughout the simulation period as shown in Figure 8(a). It also shows the reactive power generated from the diesel generator. In the islanded mode, the active power generated by the diesel generator is not enough to fulfill the power demand of the microgrid. Figures 8(b) and 8(c) shows the microgrid frequency which initially dips to a value of 57.8 Hz due to the load-generation imbalance. The frequency control from the PV generator starts at 0.1 sec which quickly regulates the frequency back to 60 Hz in 0.2 sec. Figures 8(d) and 8(e) shows the plot of the PCC voltage in p.u. It can be observed that voltage is also quickly regulated at 1 p.u. after the control is started. Figures 8(f) and 8(g) shows the active and reactive power injection from the PV inverter which regulates the frequency and voltage of the microgrid. The active power injection from the inverter, which is required to maintain the frequency at 60 Hz in both cases, is around 80 kW. However, there is a difference in the share of the PV generator and the battery energy storage while providing the required 80 kW to the microgrid. This is evident from Figure 8(h) which shows the active power from the PV, the battery, and the inverter, respectively, for both cases. In Case 1, solar irradiance is abundant at 1000 W/m2 and hence, the PV generates the maximum power of 100 kW which is more than is required to maintain the microgrid frequency. The surplus 20 kW is used to charge the battery. The negative sign in battery power means that it is a charging phase, i.e., the battery absorbs power is shown in Figure 8(h).

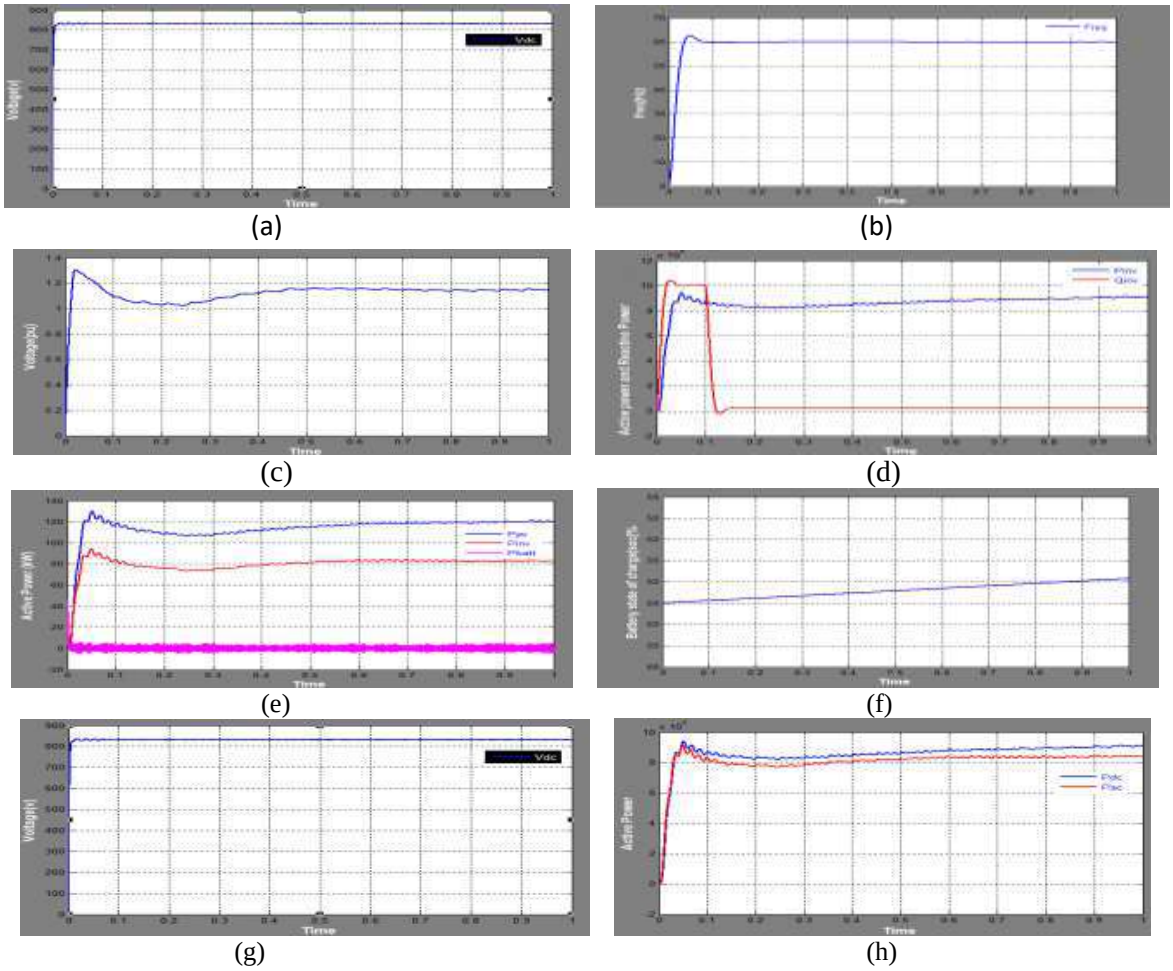

Figure 8. Results of coordinated V-f control with Solar PV including MPPT control and battery control

5. CONCLUSION

The contribution of this paper can be summarized as follows:

a. This paper proposes and presents coordinated strategies of V-f control and P-Q control, respectively, for Micro grids with PV generator and battery storage.
b. In the control strategies, the PV generator is operated at MPP, and the battery storage acts as a buffer in order to inject and absorb deficit or surplus power by using the charge/discharge cycle of the battery.

The paper contributes in demonstrating the control strategies with effective coordination between Inverter V-f (Or P-Q) control, MPPT control, and energy storage control.

a. The proposed control strategy also provides a smooth transition of PV side PQ control in grid connected Mode to V-f control in islanded mode. This is the most essential feature required in the modern Microgrid controllers.
b. The proposed control algorithms are also capable of handling the battery SOC constraint. An effective seamless transformation of controls from V-f to constant active power and voltage control at the PV side and from constant active power control to frequency control at the diesel generator is validated with satisfactory results. This feature helps the controller to adapt to the changing irradiance levels while considering the battery availability.
c. The proposed V-f control method shows a very satisfactory performance in reviving highly reduced voltage and frequency back to the nominal values in a matter of only 2 seconds. It is much faster than the diesel generator control which takes around 10 seconds to settle down. Hence, PV and battery installations might be applied effectively in restoring the microgrid frequency and the voltage at PCC after disturbances.

d. Similarly, the proposed integrated and coordinated P-Q control algorithm can be effectively used in supplying some critical loads of a microgrid with solar PV and battery.

In the present methods, the control parameters are dependent upon the PV, battery, and external grid conditions and must be re-tuned with the changing conditions. This can be overcome by using an adaptive method to obtain these parameters dynamically based on the system conditions. The adaptive control methods could be a very useful and promising future direction of this work**.**

ACKNOWLEDGEMENTS

I express my thanks to the support given by management in completing my project. I also express my sincere gratitude & deep sense of respect to Dr SVNL Lalitha for making us available all the required assistance & for her support & inspiration to carry out this project in the Institute. I would like to thank Dr SVNL Lalitha, professor who has been an inspiring guide and committed faculty who gave relief moral support in every situation of engineering career. The encouragement and support by her, especially in carrying out this project motivated me to complete this project. I am thankful to the teaching and non-teaching staff of EEE department for their direct as well as indirect help in my project. I am elated to avail my selves to this opportunity to express my deep sense of gratitude to my parents.

REFERENCES

[1] R.H. Lasseter, *"MicroGrids*", in Proc. IEEE Power Engineering Society Winter Meeting, 2002, vol. 1, pp. 305–308.
[2] S. Chowdhury, S.P. Chowdhury, and P. Crossley, "Microgrids and Active Distribution Networks", 2009, *IET Renewable Energy Series 6*.
[3] H. Saadat, *Power System Analysis*, 2nd ed. New York, NY, USA: Mc- Graw Hill, 2002.
[4] J.A.P. Lopes, C.L. Moreira, and A.G. Madureira, "Defining control strategies for Micro Grids islanded operation", *IEEE Trans. Power Syst.*, vol. 21, pp. 916–924, 2006.
[5] B. Awad, J. Wu, and N. Jenkins, "Control of distributed generation", *Electrotechn. Info. (2008)*, vol. 125/12, pp. 409–414.
[6] J.C. Vasquez, J.M. Guerrero, E. Gregorio, P. Rodriguez, R. Teodorescu, and F. Blaabjerg, *"Adaptive droop control Applied to distributed generation inverters connected to the grid"*, in Proc. 2008 IEEE ISIE, pp. 2420–2425.
[7] H. Bevrani and S. Shokoohi, "An intelligent droop control for simultaneous voltage and frequency regulation in Islanded microgrids", *IEEE Trans. Smart Grid*, vol. 4, no. 3, pp. 1505–1513, Sep. 2013.
[8] J.C. Vasquez, J.M. Guerrero, M. Savaghebi, and R. Teodorescu, "*Modelling, analysis and design of stationary Reference frame droop controlled parallel three-phase voltage source inverters"*, in Proc. 2011 IEEE 8th ICPE & ECCE, pp. 272–279.
[9] T.L. Vandoorn, B. Meersman, J.D.M. De Kooning, and L. Vandevelde, "Analogy between conventional grid contro and islanded microgrid control based on a global DC-link voltage droop", *IEEE Trans. Power Delivery*, vol. 27, no. 3, pp. 1405–1414, Jul. 2012.
[10] H. Laaksonen, P. Saari, and R. Komulainen, "Voltage and frequency control of inverter based weak LV network Microgrid", presented at the Int. Conf. Future Power Syst., Amsterdam, the Netherlands. Nov. 18, 2005.
[11] J.C. Vasquez, R.A. Mastromauro, J.M. Guerrero, and M. Liserre, "Voltage support provided by a droop-controlled Multifunctional inverter", *IEEE Trans. Ind. Electron.*, vol. 56, pp. 4510–4519, 2009.
[12] H. Li, F. Li, Y. Xu, D.T. Rizy, and J.D. Kueck, "Adaptive voltage control with distributed energy resources: Algorithm, theoretical analysis, simulation and field test verification", *IEEE Trans. Power Syst.*, vol. 25, pp. 1638–1647, Aug. 2010.
[13] H. Li, F. Li, Y. Xu, D.T. Rizy, and S. Adhikari, "Autonomous and adaptive Voltage control using multiple distributed energy resources", *IEEE Trans. Power Syst.*, vol. 28, no. 2, pp. 718–730, May 2013.
[14] L.D.Watson and J.W. Kimball, "*Frequency regulation of a microgrid using solar power*", in Proc. 2011 IEEE APEC, pp. 321–326.
[15] M.G. Molina and P.E. Mercado, *"Modeling and control of grid-connected photovoltaic energy conversion system Used as a dispersed generator"*, in Proc. 2008 IEEE/PES Transm. Distrib. Conf. Expo.: Latin America, pp. 1–8.
[16] N. Kakimoto, S. Takayama, H. Satoh, and K. Nakamura, "Power modulation of photovoltaic generator for frequency Control of power system", *IEEE Trans. Energy Conv.*, vol. 24, pp. 943–949, 2009.
[17] T. Ota, K. Mizuno, K. Yukita, H. Nakano, Y. Goto, and K. Ichiyanagi, *"Study of load frequency control for a Microgrid"*, in Proc. 2007AUPEC Power Eng. Conf., pp. 1–6.
[18] L. Xu, Z. Miao, and L. Fan, "*Coordinated control of a solar battery system in amicrogrid"*, in Proc. 2012 IEEE/PES Transm. Distrib. Conf. Expo. (T&D), pp. 1–7.
[19] M.G. Villalva, J.R. Gazoli, and E.R. Filho, "Comprehensive approach to modeling and simulation of photovoltaic Arrays", *IEEE Trans. Power Electron.*, vol. 24, no. 5, pp. 1198–1208, 2009.
[20] Y. Xu, H. Li, D.T. Rizy, F. Li, and J.D. Kueck, "*Instantaneous active and nonactive power control of distributed Energy resources with a current limiter"*, in Proc. IEEE Energy Conversion Congr. Expo. 2010, pp.3855–3861.
[21] O. Tremblay and L A. Dessaint, "Experimental validation of a battery dynamic model for EV applications", *World Electric Vehicle J.*, vol. 3, 2009.

[22] Y. Xu, F. Li, D.T. Rizy, and J.D. Kueck, "Active and nonactive power control with distributed energy resources", In *Proc. 2008 40th North American Power Symp. NAPS'08*, pp. 1–7.
[23] S. Adhikari *et al.*, "*Utility-side voltage and PQ control with inverterbased photovoltaic systems*", in Proc. 18th World Congr. IFAC, Milan, Italy, Aug. 28–Sep. 2 2011, pp. 6110–6116.

BIOGRAPHIES OF AUTHORS

Mr B V Rajanna is a student passed out from KL University from EEE Department. He obtained B.Tech degree from JNTU Kakinada in 2010 and M.Tech degree from KL University in 2015, Guntur. He had worked in different capacities in technical instituitions of higher learning over 3 years. He has over 9 publications in International Journals. His Current Research includes AMR (Automatic Meter Reading) devices, Smart Metering and Smart Grids, Micro-Grids, Renewable Energy Sources, GSM/GPRS and PLC (Power Line Carrier) Communication and Various modulation techniques such as QPSK, BPSK, ASK, FSK, OOK and GMSK.

Dr. S V N L Lalitha is working as a Professor in the Department of EEE, K L University. She obtained her M. Tech and Ph.D degrees from National Institute of Technology, Warangal, India. Obtained her B. Tech from S V University, Tirupathi. Her areas of research include power system restructuring, distribution systems, smart grids, meta heuristic techniques application to power system, wide area monitoring, control and protection.

Mr G Joga Rao was born in srikakulam, Andhra Pradesh, India, in 1983. He received B.Tech (Electrical & Electronics Engineering) degree from Kamala Institute of Technology & Science, Jawaharlal Nehru Technological University, Hyderabad, India, in 2004 and the M.Tech degree from Jawaharlal Nehru Technological University College, Hyderabad, India in 2007. Later he joined in Chirala Engineering College, Chirala, and Andhra Pradesh as an assistant professor in the department of Electrical & Electronics Engineering and serves more than 8 years. Currently pursuing his Ph.D in SunRise University, Alwar, and Rajasthan, India. His area of interest includes Power Systems, Energy Systems, and Renewable Energy Sources, Micro Grids and Smart Grids. He is a Life Member of the Indian Society for Technical Education (LMISTE).

Dr. S.K Shrivastava Received B.Tech in Electrical Engineering from Nagpur University, Nagpur in 1984, M.Tech from Indian Institute of Technology IIT(B), Bombay in 1987 and Ph.D from Allahabad Agriculture University (currently Sam Higginbottom Institute of Agriculture, Technology and Sciences, Deemed University) Allahabad, Uttar Pradesh in 2006. He has more than 27 years of teaching experience in various colleges in different capacities and acted as a technical advisior and reviewer for different programmes. His area of interest includes Energy Systems and power systems. He is a life member of different professional bodies like ISTE, Fellow the Institution of Engineers (IE), The Institution of Electronics & Telecommunication Engineers.